Ecological Indicators 101 (2019) 192–202

Contents lists available at ScienceDirect

Ecological Indicators

journal homepage: www.elsevier.com/locate/ecolind

Quantification of the ecosystem carrying capacity on China's Loess Plateau

Wei Liang[a,b,c], Bojie Fu[c,*], Shuai Wang[d], Weibin Zhang[a], Zhao Jin[e], Xiaoming Feng[c], Jianwu Yan[a,b], Yu Liu[f], Sha Zhou[g]

[a] School of Geography and Tourism, Shaanxi Normal University, Xi'an 710119, China
[b] National Demonstration Center for Experimental Geography Education, Shaanxi Normal University, Xi'an 710119, China
[c] State Key Laboratory of Urban and Regional Ecology, Research Center for Eco-Environmental Sciences, Chinese Academy of Sciences, Beijing 100085, China
[d] State Key Laboratory of Earth Surface Processes and Resource Ecology, Faculty of Geographical Science, Beijing Normal University, Beijing 100875, China
[e] State Key Laboratory of Soil Erosion and Dryland Farming on the Loess Plateau, Northwest A&F University, Yangling 712100, China
[f] Key Laboratory of Ecosystem Network Observation and Modeling, Institute of Geographical Sciences and Natural Resources Research, Chinese Academy of Sciences, Beijing 100101, China
[g] Lamont-Doherty Earth Observatory of Columbia University, Palisades, NY 10964, USA

ARTICLE INFO

Keywords:
Revegetation
Climate change
Socio-economic systems
Ecosystem carrying capacity
Sustainable water resources
Loess Plateau

ABSTRACT

Revegetation, especially afforestation, has served as an important tool for controlling desertification. However, revegetation in water-limited regions will inevitably reduce the water available for socio-economic systems, which is poorly considered in decision-making on sustainable ecosystem management. This paper proposed a framework to determine the threshold of vegetation productivity (i.e., ecosystem carrying capacity), corresponding to available water resources for ecosystems (i.e., annual precipitation minus water demand for socio-economic systems) on the Loess Plateau. The average annual ecosystem carrying capacity (ECC) during 1982–2012 is $577 \pm 124\,g\,C\,m^{-2}\,yr^{-1}$, with spatial gradients increasing from northwest to southeast. Vegetation in rocky mountain areas has the largest value of $833 \pm 200\,g\,C\,m^{-2}\,yr^{-1}$. Factorial analysis suggests that changes in precipitation and human water use contributed to 55% and 45% of the multi-decadal changes in regional ECC, respectively. Meanwhile, due to revegetation, 26 counties on the Loess Plateau, mainly in the southeast and eastern parts, have exceeded the ECC threshold during the study period. An additional 138 counties have a high potential for water competition between the ecosystems and socio-economic systems. At the regional scale, there are 9 years (~30% of the study period) during which the ECC threshold has been exceeded, especially after 1997. Considering the climate change in the future and the growing demand for water in socio-economic systems, the corresponding ECC threshold will increase by 6–36%. We believe that these findings can provide reference for policy-makers to make decisions towards ecosystem sustainability while meeting human needs for water resources.

1. Introduction

The Sustainable Development Goals are a call for action by all countries to promote prosperity while tackling climate change and environmental protection (the United Nations, 2015). It is especially urgent for the arid and semi-arid regions, which cover 41% of the Earth's land surface and are the home to more than 38% of the total population (Huang et al., 2015; Reynolds et al., 2007). Given that dry regions are confronted with more stresses from climate change, population growth and economic development than humid ones (Huang et al., 2017; Poff et al., 2016; Hartmann et al., 2013), the achievement of these goals will greatly depend on the proper allocation of water resources between ecosystems and socio-economic systems. The management of water resources for sustainable use and economic development is a difficult challenge both technically and politically (Jacobs et al., 2016). Therefore, it is necessary to carry out case studies in typical regions to provide water-related knowledge for sustainable development.

Soil erosion in the Loess Plateau of China generates some of the largest sediment yields in the world. In order to alleviate soil erosion, the Chinese government has implemented numerous revegetation practices since the 1970s (Cao, 2008; Fu et al., 2016; Liang et al., 2015), mainly including planting trees, shrubs and grass on barren land, converting cropland to forest or grassland as well as grazing prohibition. By these practices, especially large-scale afforestation in the Grain for Green (GFG) project, the Loess Plateau has exhibited the largest

* Corresponding author.
E-mail address: bfu@rcees.ac.cn (B. Fu).

https://doi.org/10.1016/j.ecolind.2019.01.020
Received 14 September 2018; Received in revised form 30 December 2018; Accepted 7 January 2019
Available online 12 January 2019

vegetation greening trend in China (Liu and Gong, 2012). However, due to depletion of deep soil water by vegetation through evapotranspiration, a series of negative effects have been reported, such as increased soil moisture deficit (Wang et al., 2011a; Cao et al., 2011), and streamflow reduction (Liang et al., 2015; Zhang et al., 2018a). Thus, the water competition between ecosystems and socio-economic systems is further aggravated (Feng et al., 2016). As the available knowledge for the optimized ecosystem management on the Loess Plateau is limited, most of the revegetation policies were not in favor of the sustainable development of ecosystems and socio-economic systems. For example, in order to eliminate the pressure on vegetation growth by grazing, local government compulsorily prohibited grazing to promote vegetation since the implementation of the GFG project in 1999 (Wang et al., 2014; Lu et al., 2016). Nevertheless, this is not beneficial for pasture growth due to the poor soil ventilation but leads to a waste of natural resources in the grasslands in the long run (Cheng et al., 2014). Meanwhile, to meet water supply demand, fuel economic development and mitigate water pressure from climate risk, policy-makers have attempted to construct large-scale structures (e.g., Liujiaxia Reservoir) and inter-basin water transfer projects (e.g., Hanjiang-Wei River Project). These large water structures, on the one hand, cost billions of dollars to design, build and maintain (Poff et al., 2016), while on the other hand, have resulted in growing water shortages in the downstream areas with profound physical, ecological and geomorphological effects on the lower reaches of the river and the estuary (Wang et al., 2010a). Therefore, with vegetation restoration, natural resource managers and policy-makers are eager to ascertain the threshold of vegetation productivity (i.e., ecosystem carrying capacity, ECC).

Several studies have estimated ECC by combining field experiments with physical-based models (Fu et al., 2012; Xia and Shao, 2008; Zhang et al., 2015). Although these studies have fully considered the interactions and feedbacks between ecological and hydrological processes, they are unlikely to couple economic effects in an effective way when upscaled from the site and hill slope levels to the regional level. Moreover, physical-based models have many uncertainties arising from model structure and parameter choice (Piao et al., 2013). Alternatively, a simple framework, which incorporates ecosystems, water systems, and socio-economic systems, has been widely used for guiding policy decisions in several case study areas, such as the Tarim River basin and Heihe River basin in China and the Murray–Darling River basin in Australia (Kandasamy et al., 2014; Liu et al., 2015; Lu et al., 2015; Zhou et al., 2015a). Recently, Feng et al. (2016) proposed an assessment framework to estimate the carbon sequestration threshold in a human-natural system, which provides a guide for revegetation on the Loess Plateau and other similar regions, yet the challenge is still daunting because of its spatial-temporal variations in precipitation (Miao et al., 2016), land surface characteristics (Liang et al., 2015) and socio-economic driving factors (Zhao et al., 2013). Furthermore, the ratio of carbon to water fluxes, i.e., water use efficiency, is considered as a fixed value in Feng et al. (2016), which actually varies among biomes (Yang et al., 2016; Zhou et al., 2015b).

Therefore, the objectives of this study are to: (1) analyze the vegetation changes in terms of types (i.e., land cover) and magnitude (i.e., leaf area index) and their impacts on the carbon and water fluxes over the Loess Plateau; (2) examine the spatial and temporal patterns of ECC and its controlling factors during the past three decades; (3) identify when and where the vegetation approached and exceeded the ECC threshold; and (4) explore the potential ECC driven by future climate change and water demand for the socio-economic systems.

2. Study area

The Loess Plateau is located in the middle reaches of the Yellow River basin in northwestern China (Fig. 1), with an approximate area of 640,000 km^2. This region is characterized by the arid and semiarid continental monsoon climate zone with sparse vegetation cover and loosely packed soil. The mean annual precipitation varies from 200 mm in the northwest to 750 mm in the southeast (Feng et al., 2012), typically occurring from June to September (60–70%) in the form of intense and rapid rainstorms.

The Loess Plateau provides nearly 90% of the sediment load and 44% of the water yield to the whole Yellow River (McVicar et al., 2007; Wang et al., 2016; Jia et al., 2017). However, due to the increased evapotranspiration with revegetation, the water yields from catchments were substantially reduced (Fu et al., 2016; Liang et al., 2015). Simultaneously, with the rapid development of the socio-economy, large amounts of surface and groundwater have been depleted by the agricultural, industrial, and domestic sector (Feng et al., 2016; Li et al., 2016). Currently, the Loess Plateau plays a critical role in food production and energy sources (e.g., coal, oil and gas) in Chinese national economic development (Zhao et al., 2013), but water resource shortages hinder regional socio-economic and ecological sustainability, and worsens the livelihood of ~100 million people who live there (Fig. S1). Therefore, there is a great need to balance water between ecosystems and socio-economic systems under the limited water resource supply.

3. Materials and methods

3.1. Estimation framework for ecosystem carrying capacity

The development needs of the socio-economic systems and of ecosystem productivity determine the water resource allocation between the two systems. Water resource demand for the socio-economic systems is mainly determined by population growth and technology development, while ecosystem productivity mainly depends on climatic factors especially precipitation and temperature (Wei et al., 2017).

Derived from the principle of conservation of mass, the water balance equation is described as follows:

$$P + R_{in} = \mathrm{ET}_t + R_{out} + \Delta G + \Delta S \quad (1)$$

where P is the precipitation (mm yr^{-1}); R_{in} is the amount of water entering the system from snowmelt and external water diversion (mm yr^{-1}); $\mathrm{ET_t}$ is the total evapotranspiration (mm yr^{-1}), and equals the sum of evapotranspiration from ecosystem (ET, mm yr^{-1}) (see Supplementary Section 1 for the details of the calculation), and from socio-economic systems ($\mathrm{ET_s}$, mm yr^{-1}), which mainly includes water for domestic use, industry and animal husbandry in this study (Supplementary Section 2); R_{out} is the amount of outflow water (mm yr^{-1}); ΔG is the changes in groundwater (mm); and ΔS is the changes in soil water storage (mm).

It was assumed that R_{in} and R_{out} were equal, i.e., their difference is negligible, at the grid scale with a spatial resolution of 1 km × 1 km. In addition, the soil depth of the Loess Plateau is 100–200 m on average, which is far greater than vegetation rooting depth (~4 m), so the groundwater storage anomaly derived from the Gravity Recovery and Climate Experiment (GRACE) satellite did not vary significantly (Feng et al., 2016). By contrast, soil moisture in this region presented a negative trend due to revegetation (Feng et al., 2016). At the annual scale, ΔG and ΔS are about two orders of magnitude smaller than precipitation and evapotranspiration. Therefore, ΔG and ΔS were assumed as zero.

When the socio-economic water demand is satisfied, the evapotranspiration from ecosystem (ET) is:

$$\mathrm{ET} = P - \mathrm{ET_s} \quad (2)$$

Gross primary productivity (GPP), which represents the total carbon assimilation from the atmosphere by vegetation, can be used as an indicator of the ecosystem productivity (Supplementary Section 3). Generally, the increase in carbon uptake (i.e., GPP) is at the cost of water consumption (i.e., ET):

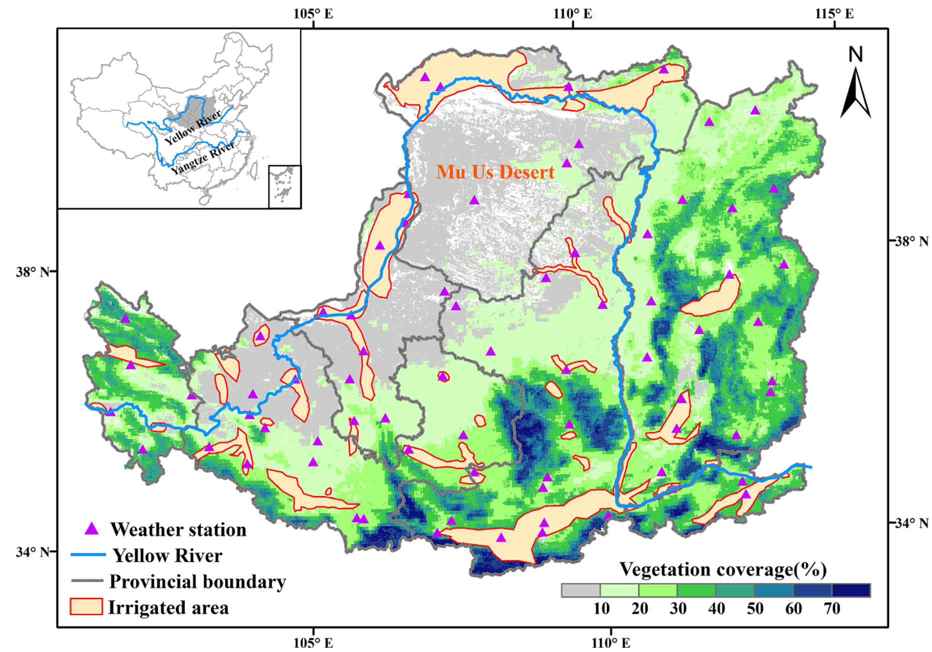

Fig. 1. Location of the Loess Plateau. The annual mean growing season (April to September) vegetation coverage from 1982 to 2012 is calculated from leaf area index.

$$\mathrm{GPP} = f\,(\mathrm{ET}) \tag{3}$$

The relationship between GPP and ET varies among different vegetation types (Zhou et al., 2014; Zhou et al., 2015b), and it was determined by linear regression for each combination of geomorphology, vegetation types and precipitation intervals (i.e., eco-hydrological regionalization in Fig. 2). The geomorphological types include six regions: loess gully regions, loess hilly and gully regions, rocky mountain, valley plain, sandy and deserted regions, and irrigated regions (Fig. S1a). The primary vegetation types are evergreen needle-leaf forest, evergreen broadleaf forest, deciduous needle-leaf forest, deciduous broadleaf forest, mixed forest, shrubland, grassland and cropland. The average annual precipitation interval was set to 50 mm (Figs. S2 and S3). Using the above relationship between GPP and ET, we calculated the ecosystem carrying capacity (ECC) as the maximum vegetation productivity (i.e., GPP), corresponding to the maximum ecosystem ET estimated by subtracting water demand for socio-economic development (domestic, industrial and animal husbandry uses) from annual precipitation.

$$\mathrm{ECC} = f\,(P - \mathrm{ET}_s) \tag{4}$$

Future ECC is also regulated by the changes in water use efficiency

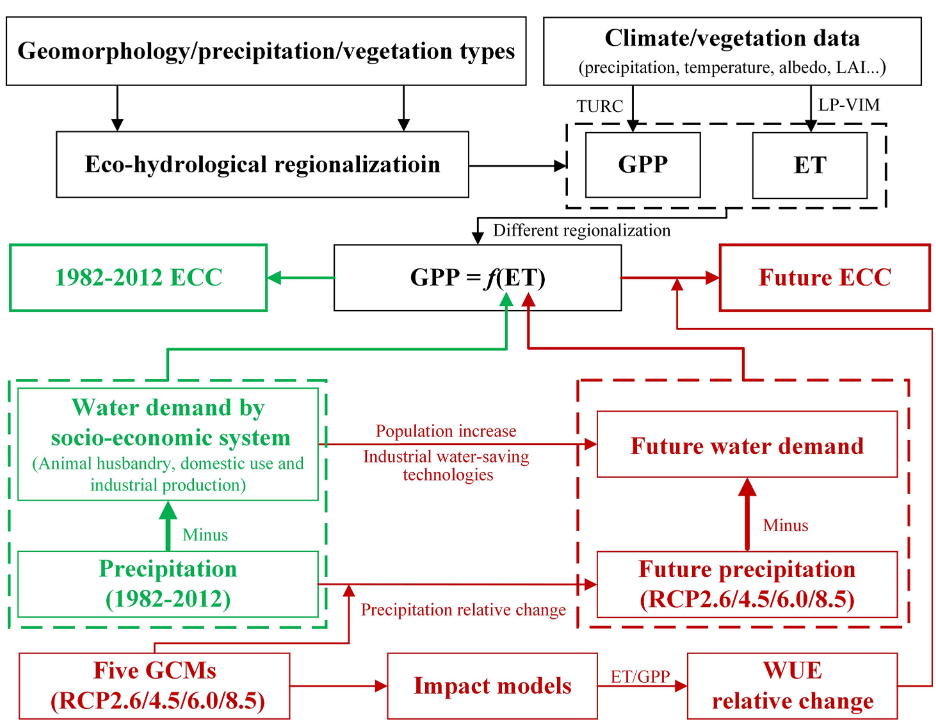

Fig. 2. Flowchart for estimating ecosystem carrying capacity (ECC).

(WUE), where WUE is defined as the ratio of GPP to ET from the Inter-Sectoral Impact Model Intercomparison Project (ISI-MIP) (Hempel et al., 2013), that is future ECC = ECC × ($WUE_{(2050s)}/WUE_{(1982\text{-}2012)}$).

In addition, to explore the extent of the GPP approaching or exceeding the ECC, we defined ϖ as the ratio of GPP to ECC, which is in the percentage form:

$$\varpi = \frac{GPP}{ECC} \times 100\% \tag{5}$$

A value of ϖ above 100% indicates that the water resource demand for socio-economic sustainable development cannot be ensured; ϖ ranges from 75% to 100% are defined as a high potential for water competition between the ecosystems and socio-economic systems.

It should be noted that the irrigated areas are not considered in this assessment, due to intensive human interference in those areas. The areas in which socio-economic water consumption is greater than 100 mm are similarly not considered in this assessment. These exclusions were done to reduce the impact of uncertainty on ECC estimation. A flowchart of ECC estimation is shown in Fig. 2.

3.2. Factorial experiments

To quantify the contributions of precipitation and water usage of the socio-economy to ECC, the differences of ECC between the simulation with only one variable varying factor (precipitation or water usage of socio-economy) and the control simulation are calculated. ECC from the control simulation in this study is the simulation forced by the mean annual (1982–2012) detrended precipitation (i.e., removing the long-term trend), mean annual social-economic water use and normal landuse covers.

3.3. Datasets

The daily meteorological data (1982–2012) at 79 stations located on and around the Loess Plateau (Fig. 1), which is mainly composed of precipitation, air pressure, relative humidity, air temperature, wind speed and sunshine duration, are obtained from the China Meteorological Data Sharing Service System. The point measurements of the stations are spatially interpolated using the method of gradient inverse distance square (GIDS) at a spatial resolution of 1 km. The annual runoff data from 1982 to 2012 at 23 hydrological stations are provided by the Yellow River Conservancy Commission (Details of these catchments can be found in Table S1 and Fig. S4).

The Global Land Surface Satellite (GLASS) leaf area index (LAI) data with a spatial resolution of 0.05 degree, and a temporal resolution of 8 days from 1982 to 2012 are obtained from Beijing Normal University (Xiao et al., 2013). The albedo (blue-sky albedo) is calculated through the black-sky shortwave albedo and white-sky shortwave albedo (Supplementary Section 1).

Land cover maps of the Loess Plateau in 1990, 2000, 2008 and 2010 with a spatial resolution of 250 m are obtained from the research of Fu et al. (2011) and the Institute of Remote Sensing and Digital Earth, Chinese Academy of Sciences. By combining automatic classification with manual checks and modification, a total number of 27 sub-classes of land cover types of the region are further grouped into six vegetation types, including forest, shrub, grassland, cropland, built-up areas and water bodies.

Associated data used for the calculation of the socio-economic water usage at the county or province scale (only for animal husbandry) mainly come from the China Statistical Yearbook, Yellow River Water Resources Bulletin, Loess Plateau Data Center, and Wang et al. (2010b) (Table S2). The water consumption for domestic use (urban and rural), industry and animal (large and small) husbandry at five-year intervals (1985, 1990, 1995, 2000, 2005 and 2010) is estimated. Generally, as the annual change in the socio-economic water use is slight, the water amount needed for maintaining the socio-economic activities on the Loess Plateau from 1982 to 2012 are obtained through simple linear interpolation. The future water demand for the 2050s (i.e., 2050–2059) is predicted based on the conditions in 2012, using the socio-economic water demand model (Supplementary Section 2).

Monthly GPP and ET (1982–2059) are from the VISIT model (Ito and Inatomi, 2012), which is driven by five global climate models (GCMs) from ISI-MIP under the different Recommended Concentration Pathways of RCP2.6, 4.5, 6.0 and 8.5 (Table S3). The two datasets are used to calculate the changes in WUE. Daily precipitation is derived from the five GCMs as well (1982–2059). Different from the Coupled Model Intercomparison Project Phase 5 (CMIP5), the output of each GCM participating in the ISI-MIP is bias corrected and downscaled to the $0.5^{\circ} \times 0.5^{\circ}$ spatial resolution (Warszawski et al., 2014). Considering the great difference in the magnitude of precipitation between ISI-MIP GCMs and spatially-interpolated (GIDS) dataset based on 79 meteorological stations (Fig. S5), the precipitation in the 2050 s was the product of the current interpolated precipitation (GIDS) and the relative precipitation change rate derived from the five GCMs.

4. Results

4.1. Vegetation changes and its impact on carbon flux and water resources

According to the available land cover data, cropland, grassland, and forest are the dominant land cover types on the Loess Plateau (~85% of the total area) (Fig. S6). During the past two decades, the land cover types of the region (especially the hilly areas in the southeast, eastern, and the central parts of the Loess Plateau) have changed dramatically driven by anthropogenic activities. This change is characterized by decreased cropland with an expansion of non-agricultural vegetation cover and built-up areas (Fig. 3). Specifically, the percentage of cropland area decreased from 34% in 1990 to 29% in 2010 (a relative change of 14%), while the built-up area increased from 2.2% to 2.8% (a relative change of 28%) over the same period. Moreover, due to afforestation, forest increased from 8% to 18% during this period.

Apart from the vegetation types, the average growing-season LAI of the whole Loess Plateau also showed a significantly upward trend from 1982 to 2012 ($0.015\,m^2\,m^{-2}\,yr^{-1}$, $p < 0.001$) (Fig. 4a), which is accompanied by an increase in the gross carbon dioxide uptake (i.e., GPP) and a proportional increase in water use (i.e., ET) (Fig. 4b). Specifically, the annual GPP of the Loess Plateau was estimated to have significantly ($p < 0.01$) increased by $4.9\,g\,C\,m^{-2}\,yr^{-2}$ from 1982 to 2012 (Fig. 4c). Moreover, consistent with the results of an earlier study (Li et al., 2017), this increasing trend in GPP mainly appears after 1999. The TURC-modeled GPP significantly increases with a rate of $7.7\,g\,C\,m^{-2}\,yr^{-2}$ in the 2000s, a figure that compares well with, although higher (lower) than the median of the eight land surface models participating in the TRENDY project (MTE) (Table S4). In exchange, the regional annual ET, which significantly increases over 71% of the study area, also experienced a significantly ($p < 0.05$) increasing trend during this period ($1.96\,mm\,yr^{-2}$) (Fig. 4d).

Fig. 5 shows the social-economic water use on the Loess Plateau during 1982–2012. Due to the population growth and economic development of the region, total water consumption increased from 2.7 billion m^3 to 10.7 billion m^3, of which the industrial sector accounted for the largest proportion (~60% after 1990) (Fig. S7a), and the largest increasing rate occurred in the middle-to-north regions (Fig. S7b). At the same time, the median of water yield capacity (runoff coefficient, runoff divided by precipitation) from the 23 catchments on the Loess Plateau significantly decreased by 0.0013 per year, and by 58% before and after 1999 (Fig. 5). Given the projected population increase and the improvement of industrial water-saving technologies, water demand for the socio-economic systems was projected to increase by 37% in the 2050 s, compared with 2012 (Fig. S7a), with a relatively stable increasing rate in most of the counties (Fig. S7c).

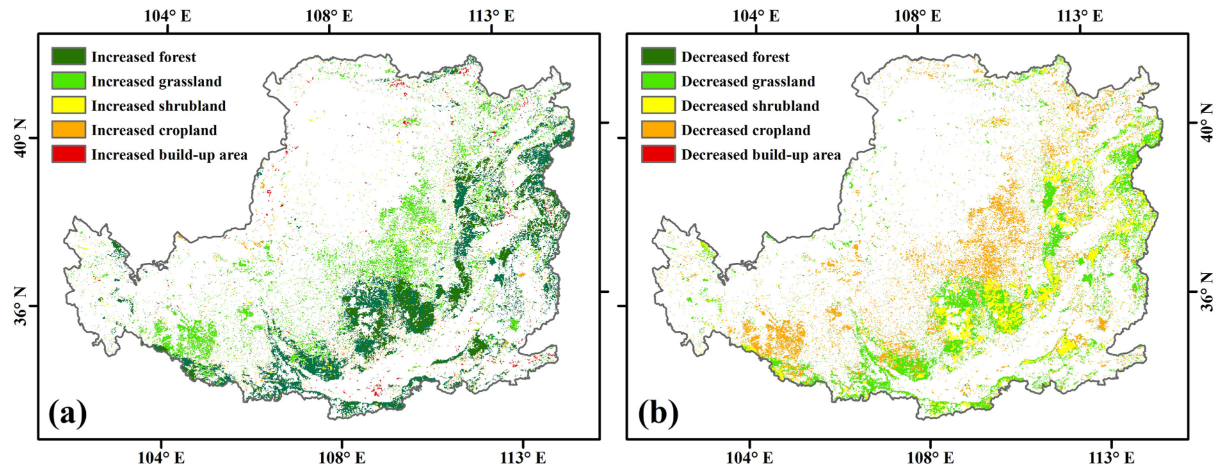

Fig. 3. Spatial distribution of: (a) increased, and (b) decreased land cover types from 1990 to 2010 over the Loess Plateau.

4.2. Spatiotemporal patterns of ecosystem carrying capacity and its controlling factors

Considering the water consumption for the socio-economic systems, ECC of the Loess Plateau over the period 1982–2012 was estimated. As shown in Fig. 6a, generally, ECC showed gradients increasing from the northwest (less than 100 $g\,C\,m^{-2}\,yr^{-1}$) to the southeast (higher than 600 $g\,C\,m^{-2}\,yr^{-1}$), with 80% of the counties falling between 200 $g\,C\,m^{-2}\,yr^{-1}$ and 860 $g\,C\,m^{-2}\,yr^{-1}$. The spatial patterns of ECC appeared to be precipitation dependent, suggesting a strong hydrological control on the spatial pattern of vegetation productivity in dry regions like the Loess Plateau (Fig. 6b). It was found that there is a precipitation inflection of ~600 mm, below which a 100 mm annual precipitation corresponds to ~200 $g\,C\,m^{-2}\,yr^{-1}$ ECC increase, and above which the ECC tended to be less influenced by precipitation. In those less precipitation-dependent areas, other factors such as temperature and solar radiation may also play an important role in determining the spatial pattern of ECC.

The average annual (1982–2012) ECC at the region scale was 577 ± 124 $g\,C\,m^{-2}\,yr^{-1}$, with the largest value of 833 ± 200 $g\,C\,m^{-2}\,yr^{-1}$ in rocky mountain areas, followed by valley plain (816 ± 244 $g\,C\,m^{-2}\,yr^{-1}$), loess gully (586 ± 133 $g\,C\,m^{-2}\,yr^{-1}$) and loess hilly and gully regions (550 ± 120 $g\,C\,m^{-2}\,yr^{-1}$) (Fig. 6c). By contrast, the vegetation in SD and IR, affected by the dry climate, has the lowest ECC (243 ± 82 $g\,C\,m^{-2}\,yr^{-1}$ and 265 ± 86 $g\,C\,m^{-2}\,yr^{-1}$, respectively).

Over the whole Loess Plateau, ECC decreased by 1.5 $g\,C\,m^{-2}$ per year from 1982 to 2012 (Fig. 7), with a contrasting trend before and after 1999 (−10.4 $g\,C\,m^{-2}\,yr^{-2}$ versus 4.0 $g\,C\,m^{-2}\,yr^{-2}$). To explore the reason for this change, we conducted factorial experiments. The factorial analysis of variance to the ECC estimates suggested that the mean annual simulated normal ECC (577 $g\,C\,m^{-2}\,yr^{-1}$) was 7% lower than that of the control simulation (619 $g\,C\,m^{-2}\,yr^{-1}$) (see Method Section 3.2), of which changes in precipitation contributed 55% of the multi-decadal changes in regional ECC, and the remaining of 45% were ascribed to changes in socio-economic water usage (Fig. 7). Moreover,

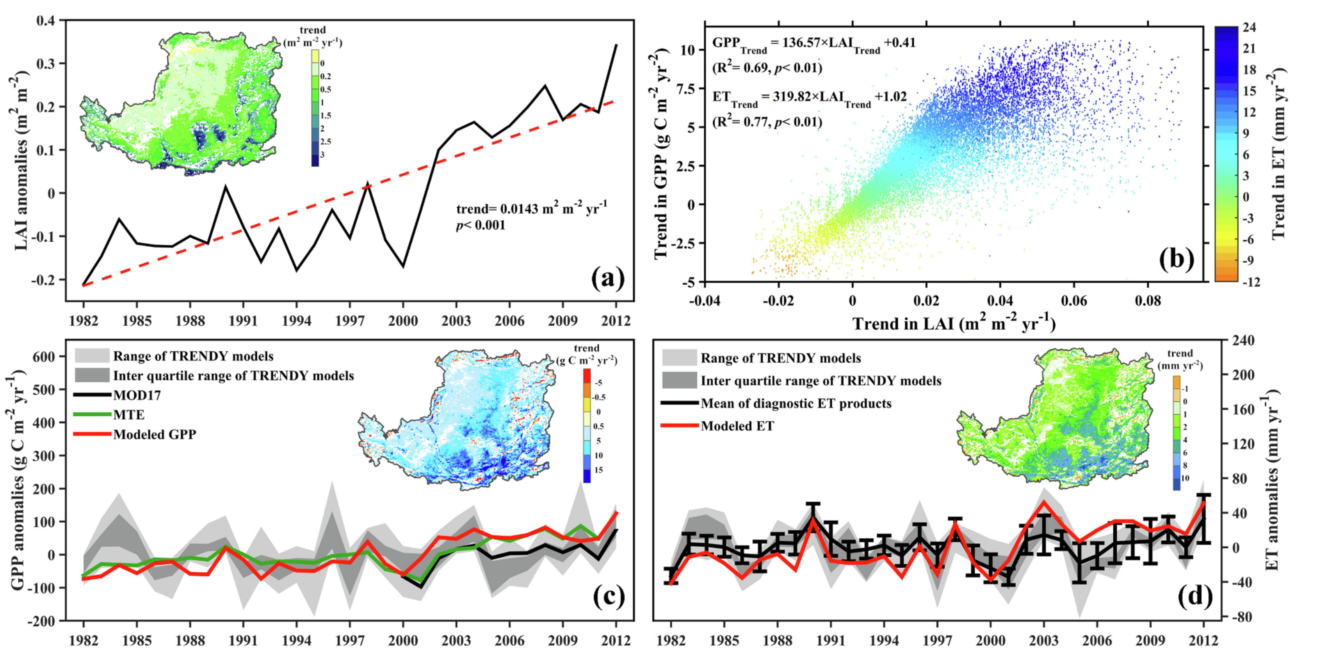

Fig. 4. Interannual changes in anomalies of: (a) growing-season LAI, (c) annual GPP, and (d) annual ET. The ensemble of the TRENDY-models in Figures c and d are eight land surface models, and error bars indicate one standard deviation within diagnostic datasets (Table S4). The insets in a, c and d show the spatial patterns of trends in growing-season LAI, annual GPP and annual ET with statistical significance at $p < 0.05$, respectively. (b) The relationship between the trends in GPP and growing-season LAI, with the color of the points corresponding to the trend in ET.

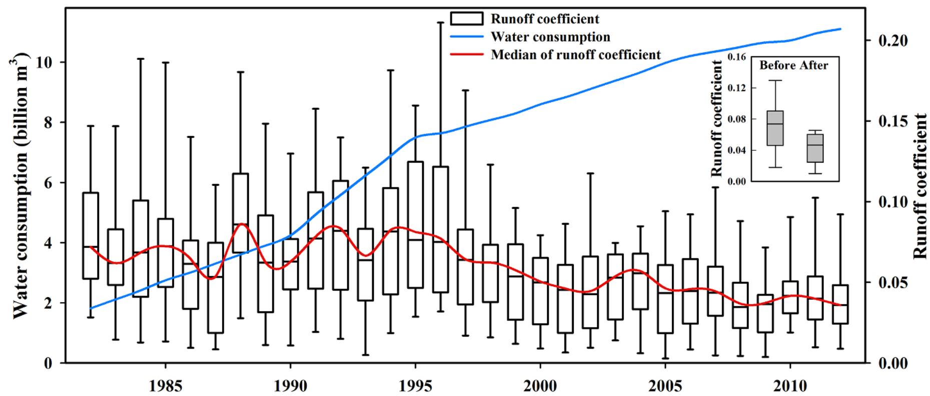

Fig. 5. Water consumption of the socio-economic systems and median of runoff coefficient (runoff/precipitation) of the 23 catchments on the Loess Plateau. The inset shows the average annual runoff coefficient before and after the implementation of the Grain for Green (GFG) project in 1999.

it is found that the effect of precipitation change is negative for each period, except the 1980s, indicating a drier climate during the past two decades. After 1999, the contribution of human effects to changes in ECC equals that of precipitation (50% versus 50%).

4.3. Overloaded vegetation on the Loess Plateau

Although the average annual ECC changes slightly throughout the whole study period (inset in Fig. 7), the rapid increase in GPP has led to a decline in capacity of additional vegetation productivity supported by available water resources, especially during recent years (i.e., increase in ϖ) (Fig. 8a). At the county level, 26 counties have exceeded the ECC threshold over the whole period (Fig. 8b). They are mainly located in the southeast and eastern parts, and 138 counties have a high potential for water resource competition (i.e., ϖ ranges from 75% to 100%) between the ecosystem and socio-economic systems. Before and after the GFG project (Fig. 8c and d), the number of counties exceeding the ECC threshold nearly tripled from 19 to 57, and the number of counties with a high potential for water resource competition increased from 101 to 168.

In the past thirty-one years, the regional mean ϖ is 89%, suggesting that the additional vegetation productivity that available water resources can support is less (11%). The interannual variability of ϖ shows that there are nine years (~30% of the study period) when the GPP is above the threshold, which first occurred in 1986 and is more concentrated after 1997 (Fig. 9). Moreover, an additional one-third of the study period has a high potential for water resource competition between the ecosystem and socio-economic systems. Similar cases can also be found in different geomorphological types, especially in rocky mountain and valley plain regions.

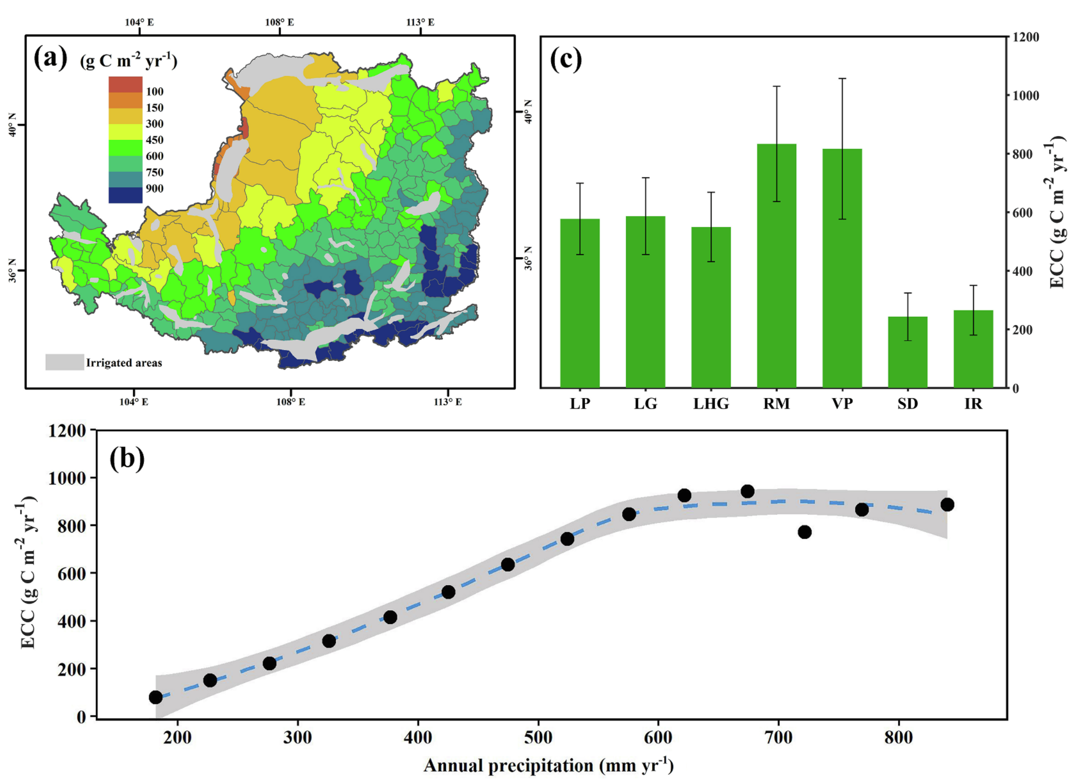

Fig. 6. (a) Spatial pattern of ECC on the Loess Plateau at the county scale over the period 1982–2012, (b) relationship between precipitation and ECC across the Loess Plateau, and (c) average annual ECC for the whole Loess Plateau and different geomorphological types. Each scatter point indicates the averaged ECC against the corresponding precipitation at an interval of 50 mm. LP, LG, LHG, RM, VP, SD, and IR correspond to the whole Loess Plateau, loess gully, loess hilly and gully, rocky mountain, valley plain, sandy desert, and irrigated regions, respectively.

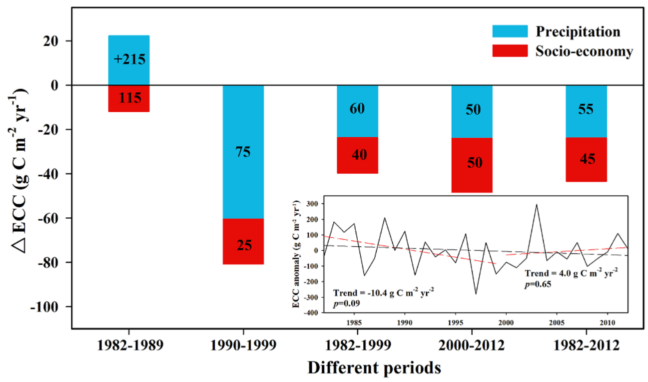

Fig. 7. Factorial contribution of changes in precipitation and social-economic water use affecting regional ECC for different periods. Numbers on the bars show the relative contributions, as an expression of percentage (%). The inset shows the temporal variation in ECC anomaly over the Loess Plateau from 1982 to 2012.

4.4. Potential ecosystem carrying capacity in the future

Compared with the historical precipitation (1982–2012), the regional mean precipitation from the five GCMs for all RCP scenarios is projected to increase by 3–14% for the 2050s (Fig. 10a), despite a large divergence for each GCM (Figs. S8 and S9). Among all RCP scenarios, precipitation under RCP8.5 has the largest increasing rate, with consistent increase across the whole study area and among different GCMs (Fig. S9). Similarly, due to the rising atmospheric CO_2 concentration, the WUE, i.e. the carbon uptake (GPP) per unit of water loss (ET), for all the four RCPs is projected to increase between 8% (RCP2.6) and 21% (RCP8.5) by mid-21st century. Compared with precipitation, the ISI-MIP projects a similar WUE magnitude change among climate models (Fig. S10), and are in good agreement on increased WUE direction across the whole study area (Fig. S11).

Considering the climate change in the future, CO_2-induced WUE, and projected increase in water demand, ECC from the ensemble mean of the five GCM can increase by 6–36% under different RCP scenarios for the 2050 s relative to 1982–2012, with the maximum being $865 \pm 56\,g\,C\,m^{-2}\,yr^{-1}$ for RCP8.5 and the minimum being $625 \pm 87\,g\,C\,m^{-2}\,yr^{-1}$ for RCP6.0 (green bars in Fig. 10a). Spatially, despite the strong divergence in projected precipitation and WUE under the four RCPs for the period 2050 s, the projected spatial distribution of ECC is almost identical for different RCP scenarios, except RCP8.5 which has larger ECC in southeastern areas than that in the other three RCP scenarios (Fig. 10b). It is shown that the vegetation will exceed the ecosystem carrying capacity threshold and have a high potential for water competition on over 14–22% and 23–25% of the area under different scenarios, respectively (Fig. 10c).

5. Discussion

5.1. Impact of revegetation on carbon and water fluxes

In natural ecosystems without or with little anthropogenic interruption, biotic components of the ecosystem evolve over time with a dynamic equilibrium to produce a stable community that can use the available resources in a sustainable way, and thus maintain the ecosystem's biodiversity (Cao et al., 2009; Dirzo and Loreau, 2005). In turn, biodiversity plays an important role in the functioning of the ecosystem and the services it provides to humanity (Bullock et al., 2011; Cardinale et al., 2012). The LAI, GPP and ET on the Loess Plateau did not systematically increase before 1999 (Fig. 4), due to the influence of the drying climate (Zhang et al., 2013). By introducing a large number of exotic species, mainly including *Robinia pseudoacacia* (a tree native to the southeastern United States) and *Hippophae rhamnoides* (a shrub native to Central and Northern Europe) (Cheng and Wan, 2002; Zhang et al., 2015), vegetation coverage (i.e., LAI) significantly increased (Fig. 4a). However, these fast-growing, deeply rooted woody plants can transpire large quantities of water compared with herbaceous plants, consuming the deep soil water as well as lowering the

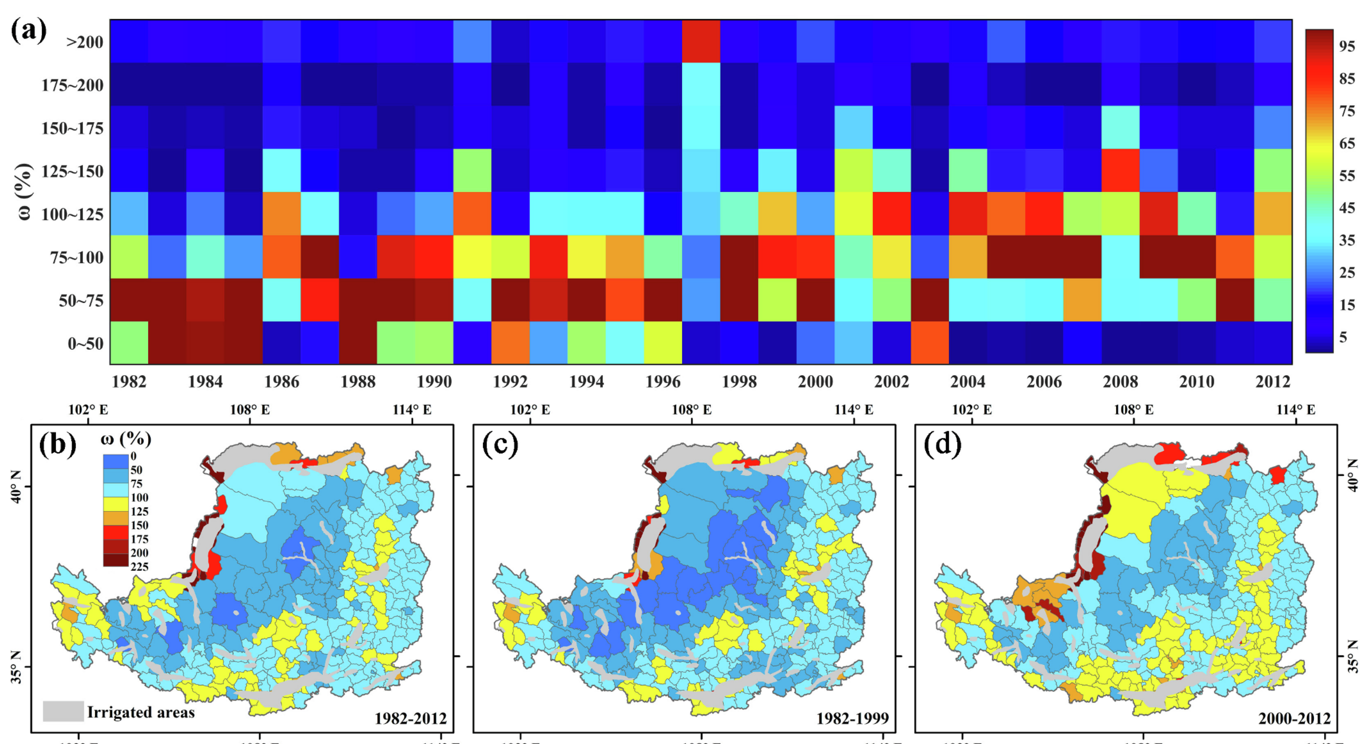

Fig. 8. (a) Numbers of counties at different ω levels over the period 1982–2012. Spatial distributions of ω at the county scale in different periods: (b) 1982–2012, (c) 1982–1999, and (d) 2000–2012.

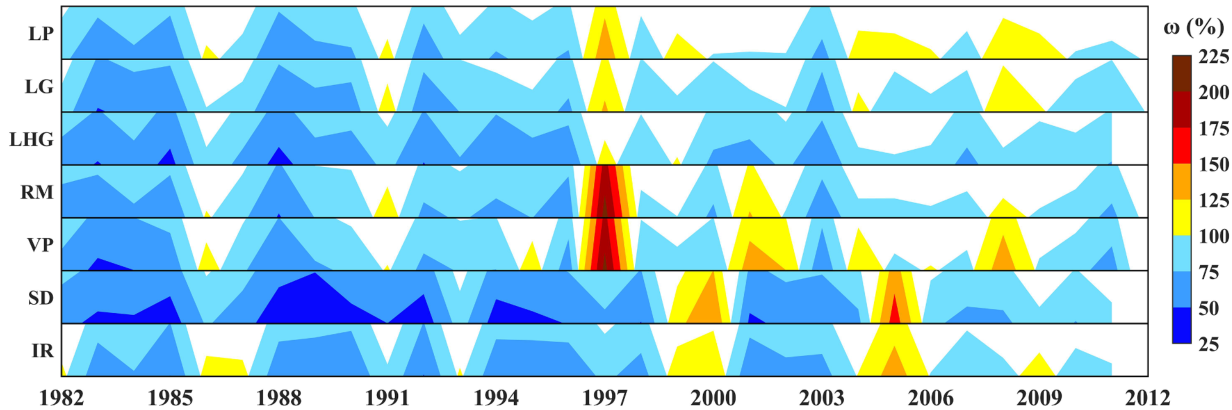

Fig. 9. Interannual variability of ω for the Loess Plateau and different geomorphologic types over the period 1982–2012. The deeper the red color, the more severe the degree of overloading (i.e., GPP > ECC); the deeper the blue color, the larger the additional vegetation can be supported. LP, LG, LHG, RM, VP, SD, and IR correspond to the whole Loess Plateau, loess gully, loess hilly and gully, rocky mountain, valley plain, sandy desert, and irrigated regions, respectively. (For interpretation of the references to colour in this figure legend, the reader is referred to the web version of this article.)

water table (Cao, 2008; Feng et al., 2017; Liang et al., 2018). On the one hand, the severe depletion of deep soil water by afforestation and long-term decreased precipitation can induce soil desiccation and ecological degradation (Deng et al., 2016; Liu et al., 2018). On the other hand, the newly planted trees can enhance carbon sequestration, but due to increasing rates of evapotranspiration (ET), afforestation can result in runoff reduction, which is overwhelmingly confirmed by many previous studies. McVicar et al. (2007), for example, have conducted a literature review on landuse-hydrology of the Loess Plateau, and found that water yield reduction varied from 10% to 70% associated with increasing afforestation area. Using a water balance database of 57 basins in the Loess Plateau, Wang et al. (2011b) suggested that the regional average annual runoff for forestlands is only 16 mm, 58% lower than that of 39 mm for non-forestlands. In other words, when coupled with the increase in water usage of socio-economy, afforestation in this vulnerable arid and semi-arid region potentially contributes to the water crisis, especially during the first few years of planting (Farley et al., 2005; Jackson et al., 2005). Therefore, when selecting sites for revegetation practices in dry regions, it should consider the water cost of carbon sequestration and plant water-use efficiency (Brown, 2014).

5.2. Comparison on the ecosystem carrying capacity

Identifying the ecosystem carrying capacity is a prerequisite for revegetation of the Loess Plateau, and some research efforts have been devoted to solving this problem (Table S5). Xia and Shao (2008), for example, predicted soil water carrying capacity on the northern Loess Plateau; the maximum plant density was 2250 plants ha^{-1} for *Caragana korshinkii* and 2800 plants ha^{-1} for *Salix psammophila*. Similarly, Fu et al. (2012) identified the optimal LAI of 1.27 for *Caragana korshinkii* and 0.7 for *Salix psammophila*. By using the water balance method, Wang and Shao (2012) estimated the maximum biomass of *Medicago sativa,* lucerne was 2600 to 3500 kg/ha in the Northern Shaanxi Loess

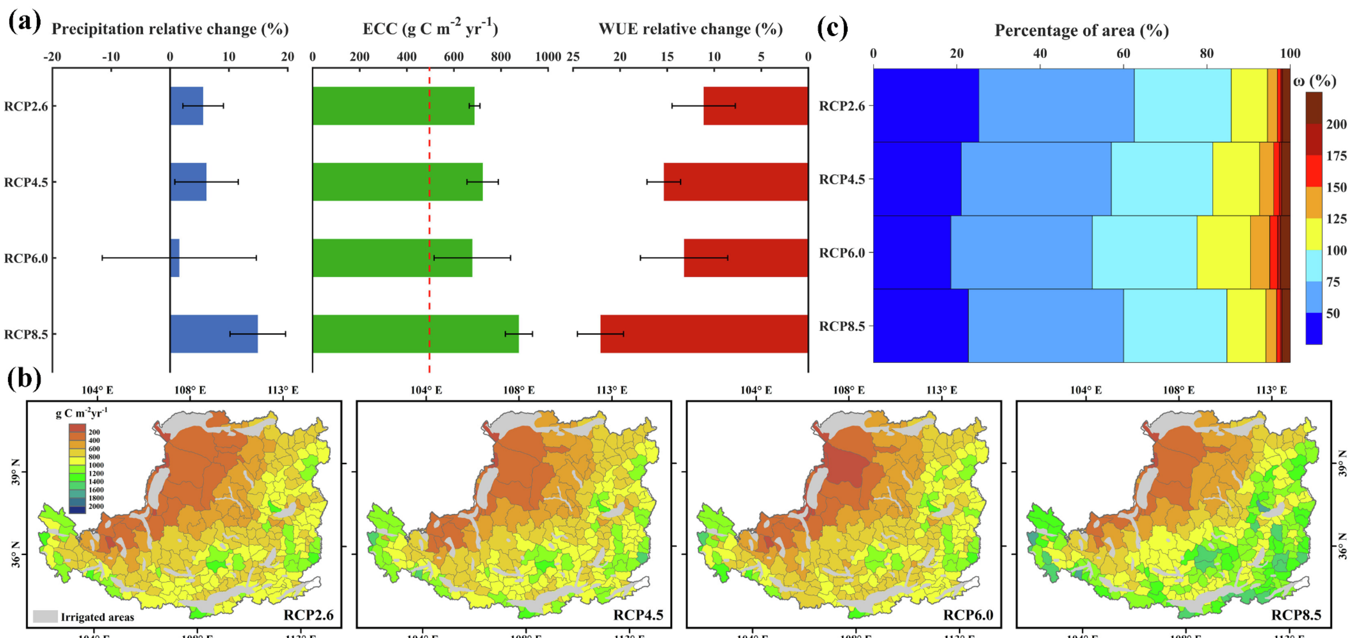

Fig. 10. ECC for the period 2050s (2050–2059) under the RCP2.6, RCP4.5, RCP6.0 and RCP8.5 scenarios. (a) Changes in average precipitation, WUE, and estimated ECC for the 2050s. Red dashed line indicates the average annual historical ECC (1982–2012); (b) spatial patterns of ECC for the period 2050s; and (c) percentage of area at different ω level for each RCP scenario. (For interpretation of the references to colour in this figure legend, the reader is referred to the web version of this article.)

Plateau. However, as these efforts mainly focused on the hill slope scale (typically 20 m long and 5 m wide) and small watersheds (< 10 km^2), or shorter periods (~ 3 years), they were not beneficial for the revegetation policy-making. Recently, Zhang et al. (2018a) estimated the optimal vegetation cover (0.43 on average) over the whole Loess Plateau based on an ecohydrological model, yet they failed to consider the impact of social activities on the eco-hydrological system. Feng et al. (2016) proposed a conceptual framework to estimate the threshold of vegetation productivity considering both ecological and socio-economic water resource demand, yet the heterogeneity of environmental factors was not fully considered. It has more great implications to quantitatively reveal the spatial distribution pattern of the ecosystem carrying capacity. Therefore, by integrating climate change data and social-economic variables (i.e., population and GDP), this study identified the maximum vegetation productivity (ECC) in a coupled human-natural system. We found that the decrease in precipitation, together with the increase in socio-economic water demand, resulted in the decline of the average ECC over the period 1982–2012, with almost equal effects (55% versus 45%) (Fig. 7). In addition, due to revegetation, 26 counties on the Loess Plateau, mainly in the southeast and eastern parts, have exceeded the ecosystem carrying capacity threshold (Fig. 8), above which the water demand for socio-economic sustainable development cannot be satisfied. Considering the climate change in the future under different RCP scenarios as well as the growing water demand of human society, the ECC during the 2050s is projected to increase by 6–36% compared with that during 1982–2012 (Fig. 10). This result contradicts the previous study by Zhang et al. (2018a), which can be attributed to the projected precipitation from GCMs. In their study, all GCMs projected a decreased precipitation during the 2050s compared with that in the past three decades (GCM projected precipitation minus spatial interpolated precipitation based on observations); by contrast, our study projected an increase of 3–14% based on a relative precipitation change rate (see Section 3.3).

5.3. Implications for ecosystem sustainable management

Observations from hydrological stations have shown that water supply from the Loess Plateau already cannot meet the water demand of socio-economic systems, especially in the last ten years (http://www.yellowriver.gov.cn/other/hhgb/). According to future planning (NDRC, 2010), 76,620 km^2 of land will be afforested from 2010 to 2030 in this region. By 2050, the Chinese government plans to invest US$9.5 billion in afforestation on the Loess Plateau (Feng et al., 2016). However, our results suggest that revegetation has promoted an increase in vegetation productivity (GPP), but this has been at the cost of water consumption (ET). Since current vegetation productivity in the Loess Plateau has approached the ECC threshold, even exceeding it in the southeast and eastern parts, continuing vegetation expansion will inevitably reduce the water available for socio-economic systems, indicating an increasing challenge for sustainable ecosystem management. Therefore, decision-makers should improve water crisis-preparation strategies given the combined demand growth (Yin et al., 2017), and reduced water supplies in the future (Zhang et al., 2018b). For the areas where vegetation productivity has approached and even exceeded the ECC threshold (Fig. 8b), some effective measures should be taken for ecosystem management. For some overloaded grassland ecosystems (Fig. S12), measures such as moderate mowing and light grazing are recommended, but the grazing season and grazing capacity should be considered. Afforestation is a poor choice for areas where annual precipitation is much lower than potential evapotranspiration (Cao et al., 2011; Deng et al., 2016), but it is a better choice for the areas where available water resources are adequate. Meanwhile, native and even exotic species that will not exacerbate soil water reductions should be prioritized for planting at appropriate densities (Cao et al., 2009).

Since the Loess Plateau includes a social component within the hydrological and ecological systems, water competition problems in dry regions should be tackled from a socioeconomic perspective (Li et al., 2018). Thus, a range of water-saving technologies and behaviors, such as increasing water recovery and utilization rates, and quitting low-value water uses, should be considered in industrial production. As agricultural irrigation accounts for the largest proportion of the total water consumption, long-term policy reforms should establish eco-compensation entitlements for farmers to avoid cropland expansion which has already resulted in groundwater overexploitation. In general, more sustainable management approaches that can ensure synergies among ecosystems, economy, and society should be promoted.

5.4. Uncertainties

It should be pointed out that the present study has some uncertainties. Currently, the assessment on ECC is made through a framework in which the maximum vegetation productivity is supported by the available water resources (i.e., the precipitation after meeting the water demand of human society). However, since vegetation growth can be constrained by many other factors such as solar radiation (Yang et al., 2015) and the available soil water resources (Laio et al., 2001), the ECC may be overestimated. Therefore, maximum vegetation productivity should be further estimated based on ecosystem optimality theory after considering the interactions among climate, soil, and vegetation (Eagleson, 1982). Moreover, the prediction of future precipitation primarily depends on GCMs; however, GCM projections are poor at capturing extreme climate events, such as droughts and storms (Rocheta et al., 2014) which have profound impacts on ecosystem carbon and water processes (Ciais et al., 2005; Jung et al., 2010) as well as socio-economic sectors (Long et al., 2014; van Dijk et al., 2013). Besides, given a lack of related observation information, CO_2-induced fertilization is simply regulated by the changes in water use efficiency. In practice, the impacts of elevated atmospheric CO_2 on vegetation productivity and hydrologic cycle are extremely complicated through stomatal behavior (Donohue et al., 2013; Ukkola et al., 2015).

Another uncertainty comes from the estimation of socio-economic water use which is averaged on each grid within the county (province for husbandry use). However, people often gather together around a city or town, and the long distances between urban areas and water resources make it difficult to meet the demand for production and living. Coupled with the water loss in the transportation processes, the water supply ability of natural ecosystems, and thus the threshold of vegetation productivity is overestimated. Most importantly, due to the lack of spatial information regarding the water supply and withdrawal, water flow among each eco-hydrological regionalization (combination of geomorphology, vegetation types and precipitation intervals) and water resource regulation by large-scale hydraulic engineering structures (e.g., reservoirs and dams) are not taken into consideration. Additionally, the lower reach of the Yellow River is the major water consumption area (mostly used for irrigation) and negligible water discharge is produced from the downstream area of the Huayuankou station (outlet of the Loess Plateau) (Liang and Liu, 2013; Wang et al., 2012). Its water resource supply mainly originates from the upper and middle reaches of the Yellow River within the Loess Plateau, which has not been considered in our estimation framework, leading to an overestimation of the threshold. Therefore, tradeoffs between local revegetation costs and downstream benefits must be taken into account in future study.

6. Conclusions

The ecological water demand increases with revegetation, resulting in a serious water competition between ecosystems and socio-economic systems on the Loess Plateau. This paper developed a framework to determine the threshold of vegetation productivity (i.e., ECC), corresponding to the maximum ecosystem ET estimated by subtracting water demand for socio-economic development from annual precipitation.

During the period 1982–2012, the average annual ECC is $577 \pm 124\,g\,C\,m^{-2}\,yr^{-1}$, which shows gradients increasing from northwest to southeast. Due to revegetation, 26 counties on the Loess Plateau, mainly in the southeast and eastern parts, have exceeded the ECC threshold during the study period. An additional 138 counties have a high potential for water competition between the ecosystems and socio-economic systems. Considering the climate change in the future and the growing demand for water in socio-economic systems, ECC during the 2050s is projected to increase by 6–36% compared with that during 1982–2012. Additionally, vegetation will exceed the ECC threshold and have a high potential for water competition with the socio-economic systems over 14–22% and 23–25% of the area under different scenarios, respectively. This study provides a valuable threshold for policy-makers to make decisions towards ecosystem sustainability while meeting human needs for water resources.

Acknowledgements

This work was funded by National Natural Science Foundation of China (41390464 and 41771118), Key Research and Development Program of China (2016YFC0501601), Natural Science Foundation of Shaanxi Province of China (2017JM4011) and Fundamental Research Funds for the Central Universities (GK201802004). Acknowledgement for the data support from Loess Plateau Data Center, National Earth System Science Data Sharing Infrastructure, National Science & Technology Infrastructure of China (http://loess.geodata.cn). All data used for this paper are properly cited and listed in the references. We are grateful to Associate Editor, Dr. Giovanni Zurlini, and two reviewers for their valuable comments and constructive suggestions. We also thank Lei Jiao for helpful discussion on the revised manuscript. The authors declare that they have no conflicts of interest.

Appendix A. Supplementary data

Supplementary data to this article can be found online at https://doi.org/10.1016/j.ecolind.2019.01.020.

References

Brown, A., 2014. Mitigation: water costs of afforestation. Nature Climate Change 4 (7) 533-533.

Bullock, J.M., Aronson, J., Newton, A.C., Pywell, R.F., Rey-Benayas, J.M., 2011. Restoration of ecosystem services and biodiversity: conflicts and opportunities. Trends Ecol. Evol. 26 (10), 541–549.

Cao, S., 2008. Why large-scale afforestation efforts in China have failed to solve the desertification problem. Environ. Sci. Technol. 42 (6), 1826–1831.

Cao, S., Chen, L., Shankman, D., et al., 2011. Excessive reliance on afforestation in China's arid and semi-arid regions: lessons in ecological restoration. Earth Sci. Rev. 104 (4), 240–245.

Cao, S., Chen, L., Yu, X., 2009. Impact of China's Grain for Green Project on the landscape of vulnerable arid and semi-arid agricultural regions: a case study in northern Shaanxi Province. J. Appl. Ecol. 46 (3), 536–543.

Cardinale, B.J., Duffy, J.E., Gonzalez, A., et al., 2012. Biodiversity loss and its impact on humanity. Nature 486 (7401), 59.

Cheng, J.M., Jing, Z.B., Jin, J.W., et al., 2014. Restoration and utilization mechanism of degraded grassland in the semi-arid region of Loess Plateau. Scientia Sinica Vitae 2014 (44), 267–279 (in Chinese with abstract in English).

Cheng, J., Wan, H., 2002. Vegetation Constructions and Water Constructions and Water Conservation in the Loess Plateau in China. Chinese Forestry Publishing Press, Beijing, pp. 208–340 (in Chinese).

Ciais, P., Reichstein, M., Viovy, N., et al., 2005. Europe-wide reduction in primary productivity caused by the heat and drought in 2003. Nature 437 (7058), 529–533.

Deng, L., Yan, W., Zhang, Y., Shangguan, Z., 2016. Severe depletion of soil moisture following land-use changes for ecological restoration: evidence from northern China. Forest Ecol. Manage. 366, 1–10.

Dirzo, R., Loreau, M., 2005. Biodiversity science evolves. Science 310 (5750), 943.

Donohue, R.J., Roderick, M.L., McVicar, T.R., Farquhar, G.D., 2013. Impact of CO_2 fertilization on maximum foliage cover across the globe's warm, arid environments. Geophys. Res. Lett. 40 (12), 3031–3035.

Eagleson, P.S., 1982. Ecological optimality in water-limited natural soil-vegetation systems: 1. Theory and hypothesis. Water Resour. Res. 18 (2), 325–340.

Farley, K.A., Jobbágy, E.G., Jackson, R.B., 2005. Effects of afforestation on water yield: a global synthesis with implications for policy. Global Change Biol. 11 (10), 1565–1576.

Feng, X., Fu, B., Piao, S., et al., 2016. Revegetation in China's Loess Plateau is approaching sustainable water resource limits. Nature Climate Change 6 (11), 1019–1022.

Feng, X., Li, J., Cheng, W., et al., 2017. Evaluation of AMSR-E retrieval by detecting soil moisture decrease following massive dryland re-vegetation in the Loess Plateau, China. Remote Sens. Environ. 196, 253–264.

Feng, X.M., Sun, G., Fu, B.J., et al., 2012. Regional effects of vegetation restoration on water yield across the Loess Plateau, China. Hydrol. Earth System Sci. 16 (8), 2617–2628.

Fu, B., Liu, Y., Lü, Y., et al., 2011. Assessing the soil erosion control service of ecosystems change in the Loess Plateau of China. Ecol. Complexity 8 (4), 284–293.

Fu, B., Wang, S., Liu, Y., et al., 2016. Hydrogeomorphic ecosystem responses to natural and anthropogenic changes in the Loess Plateau of China. Annu. Rev. Earth Planet. Sci. 45 (1), 223–243.

Fu, W., Huang, M., Gallichand, J., Shao, M., 2012. Optimization of plant coverage in relation to water balance in the Loess Plateau of China. Geoderma 173–174, 134–144.

Hartmann, D.L., et al., 2013. In: Climate Change 2013: The Physical Science Basis. IPCC, Cambridge University Press, pp. 159–254.

Hempel, S., Frieler, K., Warszawski, L., Schewe, J., Piontek, F., 2013. A trend-preserving bias correction -the ISI-MIP approach. Earth System Dyn. 4 (2), 219–236.

Huang, J., Yu, H., Dai, A., Wei, Y., Kang, L., 2017. Drylands face potential threat under 2 °C global warming target. Nature Climate Change 7 (6), 417–422.

Huang, J., Yu, H., Guan, X., Wang, G., Guo, R., 2015. Accelerated dryland expansion under climate change. Nature Climate Change 6 (2), 166–171.

Ito, A., Inatomi, M., 2012. Use of a process-based model for assessing the methane budgets of global terrestrial ecosystems and evaluation of uncertainty. Biogeosci. Discuss. 9 (2), 759–773.

Jackson, R.B., Jobbágy, E.G., Avissar, R., et al., 2005. Trading water for carbon with biological carbon sequestration. Science 310 (5756), 1944–1947.

Jacobs, K., Lebel, L., Buizer, J., et al., 2016. Linking knowledge with action in the pursuit of sustainable water-resources management. Proc. Natl. Acad. Sci. U.S.A. 113 (17), 4591–4596.

Jia, Y., An, X., Wang, H., 2017. Research on Key Technology of Water Resources Management in the Yellow River [in Chinese]. Science Press, Beijing, China.

Jung, M., Reichstein, M., Ciais, P., et al., 2010. Recent decline in the global land evapotranspiration trend due to limited moisture supply. Nature 467 (7318), 951–954.

Kandasamy, J., Sounthararajah, D., Sivabalan, P., et al., 2014. Socio-hydrologic drivers of the pendulum swing between agricultural development and environmental health: a case study from Murrumbidgee River basin, Australia. Hydrol. Earth System Sci. Discuss. 10 (6), 7197–7233.

Laio, F., Porporato, A., Ridolfi, L., Rodriguez-Iturbe, I., 2001. Plants in water-controlled ecosystems: active role in hydrologic processes and response to water stress: II. Probabilistic soil moisture dynamics. Adv. Water Resour. 24 (7), 707–723.

Li, J., Peng, S., Li, Z., 2017. Detecting and attributing vegetation changes on China's Loess Plateau. Agric. Forest Meteorol. 247, 260–270.

Li, S., Liang, W., Fu, B., et al., 2016. Vegetation changes in recent large-scale ecological restoration projects and subsequent impact on water resources in China's Loess Plateau. Sci. Total Environ. 569–570, 1032–1039.

Li, X., Cheng, G., Ge, Y., et al., 2018. Hydrological cycle in the Heihe River Basin and its implication for water resource management in endorheic basins. J. Geophys. Res. Atmos. 123 (2), 890–914.

Liang, H., Xue, Y., Li, Z., et al., 2018. Soil moisture decline following the plantation of Robinia pseudoacacia forests: evidence from the Loess Plateau. Forest Ecol. Manage. 412, 62–69.

Liang, L., Liu, Q., 2013. Streamflow sensitivity analysis to climate change for a large water-limited basin. Hydrol. Processes 28 (4), 1767–1774.

Liang, W., Bai, D., Wang, F., et al., 2015. Quantifying the impacts of climate change and ecological restoration on streamflow changes based on a Budyko hydrological model in China's Loess Plateau. Water Resour. Res. 51 (8), 6500–6519.

Liu, D., Tian, F., Lin, M., Sivapalan, M., 2015. A conceptual socio-hydrological model of the co-evolution of humans and water: case study of the Tarim River basin, western China. Hydrol. Earth System Sci. 19 (2), 1035–1054.

Liu, S., Gong, P., 2012. Change of surface cover greenness in China between 2000 and 2010. Chin. Sci. Bull. 57 (22), 2835–2845.

Liu, Y., Miao, H.-T., Huang, Z., et al., 2018. Soil water depletion patterns of artificial forest species and ages on the Loess Plateau (China). Forest Ecol. Manage. 417, 137–143.

Long, D., Shen, Y., Sun, A., et al., 2014. Drought and flood monitoring for a large karst plateau in Southwest China using extended GRACE data. Remote Sens. Environ. 155 (1), 145–160.

Lu, H.L., Zhou, L.H., Chen, Y., et al., 2016. Adaptive strategy of peasant households and its influencing factors under the grazing prohibition policy in Yanchi county, Ningxia Hui autonomous region. Acta Ecol. Sinica 36 (17), 5601–5610 (in Chinese with abstract in English).

Lu, Z., Wei, Y., Xiao, H., et al., 2015. Evolution of the human-water relationships in Heihe River basin in the past 2000 years. Hydrol. Earth System Sci. Discuss. 12 (1), 1059–1091.

McVicar, T.R., Li, L., Van Niel, T.G., et al., 2007. Developing a decision support tool for China's re-vegetation program: Simulating regional impacts of afforestation on average annual streamflow in the Loess Plateau. Forest Ecol. Manage. 251 (1–2), 65–81.

Miao, C., Sun, Q., Duan, Q., Wang, Y., 2016. Joint analysis of changes in temperature and precipitation on the Loess Plateau during the period 1961–2011. Climate Dyn. 47 (9–10), 3221–3234.

National Development and Reform Commission (NDRC), Ministry of Water Resources,

Ministry of Agriculture and National Forestry Bureau, 2010. Brief of Comprehensive Management in the Loess Plateau (2010–2030) [in Chinese]. pp. 39.
Piao, S., Sitch, S., Ciais, P., et al., 2013. Evaluation of terrestrial carbon cycle models for their response to climate variability and to CO_2 trends. Global Change Biol. 19 (7), 2117–2132.
Poff, L.R., Brown, C.M., Grantham, T.E., et al., 2016. Sustainable water management under future uncertainty with eco-engineering decision scaling. Nature Climate Change 6 (1), 25–34.
Reynolds, J.F., Smith, D.M.S., Lambin, E.F., et al., 2007. Global desertification: building a science for dryland development. Science 316 (5826), 847–851.
Rocheta, E., Sugiyanto, M., Johnson, F., Evans, J., Sharma, A., 2014. How well do general circulation models represent low-frequency rainfall variability? Water Resour. Res. 50 (3), 2108–2123.
Ukkola, A.M., Prentice, I.C., Keenan, T.F., et al., 2015. Reduced streamflow in water-stressed climates consistent with CO_2 effects on vegetation. Nature Climate Change 6 (1), 75–78.
United Nations (UN), 2015. Transforming our World: the 2030 Agenda for Sustainable Development Annex A/RES/70/1, https://sustainabledevelopment.un.org/post2015/transformingourworld.
van Dijk, A.I.J.M., Beck, H.E., Crosbie, R.S., et al., 2013. The Millennium Drought in southeast Australia (2001–2009): natural and human causes and implications for water resources, ecosystems, economy, and society. Water Resour. Res. 49 (2), 1040–1057.
Wang, H., Bi, N., Saito, Y., et al., 2010a. Recent changes in sediment delivery by the Huanghe (Yellow River) to the sea: causes and environmental implications in its estuary. J. Hydrol. 391 (3), 302–313.
Wang, H., Jia, Y.W., Wang, J.H., et al., 2010b. Evolutionary Laws of Water Resources in the Yellow River Basin [in Chinese], first ed. Science Press, Beijing, China.
Wang, S., Fu, B., Piao, S., et al., 2016. Reduced sediment transport in the Yellow River due to anthropogenic changes. Nature Geosci. 9 (1), 38–41.
Wang, S., Yan, M., Yan, Y., Shi, C., He, L., 2012. Contributions of climate change and human activities to the changes in runoff increment in different sections of the Yellow River. Quaternary Int. 282, 66–77.
Wang, X.J., Zhou, L.H., Shi, M.J., 2014. Sustainable development of a rural economy under grazing prohibition in a desertification control region and agro-pastoral transitional zone. Resour. Sci. 36 (10), 2166–2173 (in Chinese with abstract in English).
Wang, Y., Shao, M., 2012. Vegetation soil water carrying capacity of artificial pasture in loess region in Northern Shaanxi, China [in Chinese]. Trans. Chin. Soc. Agric. Eng. 28 (18), 134–141.
Wang, Y., Shao, M., Zhu, Y., Liu, Z., 2011a. Impacts of land use and plant characteristics on dried soil layers in different climatic regions on the Loess Plateau of China. Agric. Forest Meteorol. 151 (4), 437–448.
Wang, Y., Yu, P., Feger, K.H., et al., 2011b. Annual runoff and evapotranspiration of forestlands and non-forestlands in selected basins of the Loess Plateau of China. Ecohydrology 4 (2), 277–287.
Warszawski, L., Frieler, K., Huber, V., et al., 2014. The Inter-Sectoral Impact Model Intercomparison Project (ISI-MIP): project framework. Proc. Natl. Acad. Sci. U.S.A. 111 (9), 3228–3232.
Wei, Y.P., et al., 2017. Theory and Practice of Socio-hydrology [in Chinese]. Science Press, Beijing, China.
Xia, Y.Q., Shao, M., 2008. Soil water carrying capacity for vegetation: a hydrologic and biogeochemical process model solution. Ecol. Modell. 214 (2), 112–124.
Xiao, Z., Liang, S., Wang, J., et al., 2013. Use of general regression Neural Networks for generating the GLASS leaf area index product from time-series MODIS surface reflectance. IEEE Trans. Geosci. Remote Sens. 52 (1), 209–223.
Yang, Y., Donohue, R.J., McVicar, T.R., Roderick, M.L., 2015. An analytical model for relating global terrestrial carbon assimilation with climate and surface conditions using a rate limitation framework. Geophys. Res. Lett. 42 (22), 9825–9835.
Yang, Y., Guan, H., Batelaan, O., et al., 2016. Contrasting responses of water use efficiency to drought across global terrestrial ecosystems. Scientific Rep. 6, 23284.
Yin, Y., Tang, Q., Liu, X., Zhang, X., 2017. Water scarcity under various socio-economic pathways and its potential effects on food production in the Yellow River basin. Hydrol. Earth System Sci. 21 (2), 1–29.
Zhang, B., Wu, P., Zhao, X., Wang, Y., Gao, X., 2013. Changes in vegetation condition in areas with different gradients (1980–2010) on the Loess Plateau, China. Environ. Earth Sci. 68 (8), 2427–2438.
Zhang, S., Yang, D., Yang, Y., et al., 2018a. Excessive afforestation and soil drying on China's Loess Plateau. J. Geophys. Res.: Biogeosciences.
Zhang, S., Yang, Y., Mcvicar, T.R., Yang, D., 2018b. An analytical solution for the impact of vegetation changes on hydrological partitioning within the Budyko framework. Water Resour. Res. 54 (1), 519–537.
Zhang, Y., Huang, M., Lian, J., 2015. Spatial distributions of optimal plant coverage for the dominant tree and shrub species along a precipitation gradient on the central Loess Plateau. Agric. Forest Meteorol. 206, 69–84.
Zhao, G., Mu, X., Wen, Z., Wang, F., Gao, P., 2013. Soil erosion, conservation, and eco-environment changes in the Loess Plateau of China. Land Degrad. Development 24 (5), 499–510.
Zhou, S., Huang, Y., Wei, Y., Wang, G., 2015a. Socio-hydrological water balance for water allocation between human and environmental purposes in catchments. Hydrol. Earth System Sci. 19 (8), 3715–3726.
Zhou, S., Yu, B., Huang, Y., Wang, G., 2014. The effect of vapor pressure deficit on water use efficiency at the subdaily time scale. Geophys. Res. Lett. 41 (14), 5005–5013.
Zhou, S., Yu, B., Huang, Y., Wang, G., 2015b. Daily underlying water use efficiency for AmeriFlux sites. J. Geophys. Res. Biogeosci. 120 (5), 887–902.